Proc. Natl. Acad. Sci. USA
Vol. 91, pp. 11854–11858, December 1994
Biophysics

Light-induced isomerization causes an increase in the chromophore tilt in the M intermediate of bacteriorhodopsin: A neutron diffraction study

(purple membrane/retinal/conformational change)

T. HAUSS*, G. BÜLDT†, M. P. HEYN‡, AND N. A. DENCHER§

Biophysics Group, Department of Physics, Freie Universität Berlin, Arnimallee 14, D-14195 Berlin, Germany

Communicated by M. A. El-Sayed, August 12, 1994

ABSTRACT **Bacteriorhodopsin (BR) was regenerated with two selectively deuterated retinals, one with 11 deuterons in the β-ionone ring (D11) and the other with 5 deuterons (D5) at the end of the polyene chain closest to the Schiff base at carbon atoms C-14, C-15, and C-20. Both label positions (centers of deuteration) were obtained from difference Fourier maps of projections onto the plane of the membrane by neutron diffraction at 90 K, both in the light-adapted ground-state BR_{568} and in the photocycle intermediate M_{412}. To retard the decay of M_{412}, purple membrane films were soaked in 0.1 M or 1 M guanidine hydrochloride at pH 9.6. M_{412} was produced by illuminating oriented membrane films at physiological temperature (278 K), followed by rapid cooling to 90 K in the absence of light. The results show that in the projected structure the ring position is unaltered during the transition from BR_{568} to M_{412}, whereas the position of the D5 label shifts by 1.4 ± 0.9 Å toward the ring. The shortened interlabel distance in the projected structure for the M_{412} state implies that as a result of the all-*trans*/13-*cis* isomerization, the C-5 to C-13 part of the polyene chain tilts out of the plane of the membrane toward the cytoplasm by about 11° ± 6°. Pairwise comparison of data sets with the same retinal for the two photocycle states M_{412} and BR_{568} leads to four difference-density maps for the protein, which are in agreement with previous work. They show changes in the protein density near helices G and F.**

The functional cycle of the light-driven proton pump bacteriorhodopsin (BR) is accompanied by structural changes in both the chromophore and the protein. The light-adapted ground-state BR_{568} has an all-*trans* chromophore with a protonated positively charged Schiff base. The M_{412} state has a 13-*cis* chromophore and is the only intermediate with a deprotonated, uncharged Schiff base. M_{412} is the key intermediate of the photocycle. Recently direct evidence for structural changes of the protein in the M_{412} state has been obtained by neutron, x-ray, and electron diffraction (1–6). Small density changes of about 7% of the density of an α-helix are mainly located near helices G (in all studies), B, and F. It is likely that during the transition from BR_{568} to M_{412} the chromophore has changed its position and/or orientation either as a direct consequence of the isomerization or as the combined result of isomerization and protein rearrangement. In previous work, we determined the in-plane arrangement of the chromophore by performing neutron diffraction experiments with three specifically deuterated retinals (7–9). These results have been confirmed by x-ray diffraction with heavy atom-labeled retinals (10) and were incorporated into the structural model (11). In addition, from lamellar neutron diffraction, the Schiff base and the β-ionone ring were located in the direction perpendicular to the membrane in the dark-adapted ground state (12). Here, we have investigated by neutron diffraction whether the deuterated labels in the β-ionone ring and near the Schiff base, respectively, change their positions between BR_{568} and M_{412}. To collect neutron diffraction data of sufficient accuracy, 3 days of measuring time were necessary for every sample in each state. Purple membrane film samples were prepared at pH 9.6 in the presence of guanidine hydrochloride (Gdn·HCl). Under these conditions the decay of M_{412} is slowed down, allowing its steady-state accumulation at physiological temperatures in the presence of light and its subsequent trapping at 90 K in the absence of light. The data obtained clearly reveal that during the functional cycle of BR, the end of the polyene chain close to the Schiff base, which is the active center of this proton pump, changes its position.

METHODS

Sample Preparation and Neutron Diffraction. Purple membrane was isolated from *Halobacterium salinarium* strain JW5, a retinal-deficient mutant. Cultivation of cells and *in vivo* regeneration of bacterioopsin with specifically deuterated and perprotonated retinal were performed as described (8, 9). The two specifically deuterated retinals are the D11-retinal with 11 deuterons in the β-ionone ring and the D5-retinal, labeled near the Schiff base end (see Fig. 1 *Insets*). Synthesis and characterization have been described (8, 9). Four samples of about 120 mg of purple membrane each were prepared as multilayer films at pH 9.6 in the presence of 1 M Gdn·HCl and measured at 86% relative humidity (2). For the D5-BR_{568} purple membranes, two samples at 1 and 0.1 M Gdn·HCl were prepared, and no intensity differences were detected. The mosaic spread of these films was <10° full-width at half-maximum. The light-adapted ground-state BR_{568} and the photocycle intermediate M_{412} were both measured at 90 K and generated as described (2). M_{412} was first formed to an extent of 100% at room temperature under steady illumination and cooled to 5°C. Subsequently, the sample was trapped in M_{412} by cooling to 90 K in the absence of light. The purpose of this procedure was to prepare M_{412} at a physiological temperature, thereby preventing the trapping of M in an artificial inactive low-temperature form. The BR_{568} sample was obtained in the same way, except that before cooling to 90 K it was allowed to decay back completely to the light-adapted ground state. In-plane neutron

The publication costs of this article were defrayed in part by page charge payment. This article must therefore be hereby marked "*advertisement*" in accordance with 18 U.S.C. §1734 solely to indicate this fact.

Abbreviations: BR, bacteriorhodopsin; Gdn·HCl, guanidine hydrochloride.

*Present address: Hahn-Meitner-Institut, Glienicker Strasse 100, D-14109 Berlin, Germany.
†Present address: Forschungszentrum Jülich, Department of Structural Biology, D-52425 Jülich, Germany.
‡To whom reprint requests should be addressed.
§Present address: Institute of Biochemistry, Technische Hochschule Darmstadt, Petersenstrasse 22, D-64285 Darmstadt, Germany.

diffraction patterns were recorded on the D16 diffractometer of the Institute Laue-Langevin (Grenoble) at a wavelength of 4.5 Å by several $\theta - 2\theta$ scans in about 60 h (see Fig. 1). To minimize systematical errors, each deuterated sample was compared with a perprotonated one that was prepared and measured in parallel. The statistical error in intensity, averaged over the reflections from (1,0) to (5,1), was 3.5% [excluding (3,0)]. The integrated intensities were derived by fitting one or more Gaussians with a linear background to the measured data points (see Table 1). Amplitudes were derived from these intensities as described (2, 8), with phases and intensity ratios for overlapping reflections from electron microscopy (13).

RESULTS

Both label positions (centers of deuteration) were determined in M_{412} and in the light-adapted ground-state BR_{568}. This requires eight sets of diffraction data. The complete set of intensity data is presented in Table 1. Since these label positions have been determined previously in the dark-adapted state BR_{568} (8, 9) containing a mixture of 13-*cis*- and all-*trans*-retinal, only the four data sets for the M_{412} state are shown in Fig. 1. In Fig. 1 the data for D11-retinal (*A*) and D5-retinal (*B*) in M_{412} are compared with those of perprotonated retinal. To facilitate the comparison, the data sets of the H11- and H5-retinal BR are slightly shifted to the right. The (*h,k*) reflections of Fig. 1 were indexed on a hexagonal lattice. The measured unit cell dimension in the light-adapted BR_{568} state shrinks from 62.2 Å at room temperature to 61.6 Å at 90 K. In M_{412}, the unit cell dimension is 0.1–0.2 Å larger than that in BR_{568} at the same temperature. The same observations were made in other diffraction experiments (1, 2, 4, 5) except in the electron diffraction work by Glaeser *et al.* (14) for glucose-embedded purple membrane, in which the lattice constant changed neither by cooling nor between BR_{568} and M_{412}. The temperature factors and widths of the reflections did not change between the BR_{568} and M_{412} states. We thus observe, in agreement with refs. 1–6 and 14, a lattice of excellent quality in M_{412} (Fig. 1) and cannot confirm reports suggesting a great loss in lattice quality (15–17).

Table 1. Unscaled Lorentz-corrected intensities for the eight diffraction measurements

	D11-BR_{568}		D11-M_{412}		D5-BR_{568}		D5-M_{412}	
h,k	Prot	D11	Prot	D11	Prot	D5	Prot	D5
1,0	727	714	541	656	784	914	741	844
1,1	3640	3697	3362	3541	4749	5372	4241	4977
2,0	1637	1916	1676	2054	2140	2437	2161	2528
2,1	991	1150	1157	1335	1481	1395	1521	1556
3,0	79	92	117	109	50	76	104	91
2,2	680	608	614	582	813	807	787	754
3,1	1025	1166	1231	1360	1282	1124	1425	1334
4,0	488	348	368	288	621	709	450	454
3,2	765	828	1047	1101	949	991	1337	1480
4,1	1042	803	806	568	1334	1395	886	1006
5,0	827	863	975	953	995	936	1211	1316
4,2	1538	1310	1815	1599	1682	1781	2136	2333
5,1	561	417	682	558	707	665	785	789
6,0	444	616	456	590	978	983	844	626
4,3	2878	2792	2962	2835	3368	3573	3651	4099
5,2	1005	1005	947	999	1168	1240	1088	1072
6,1	413	515	495	592	592	720	535	655
5,3	956	1109	1157	1187	1170	1277	1262	1360
6,2	234	269	277	224	313	256	335	321
7,1	705	649	859	693	1100	890	1054	1030

Prot, protonated.

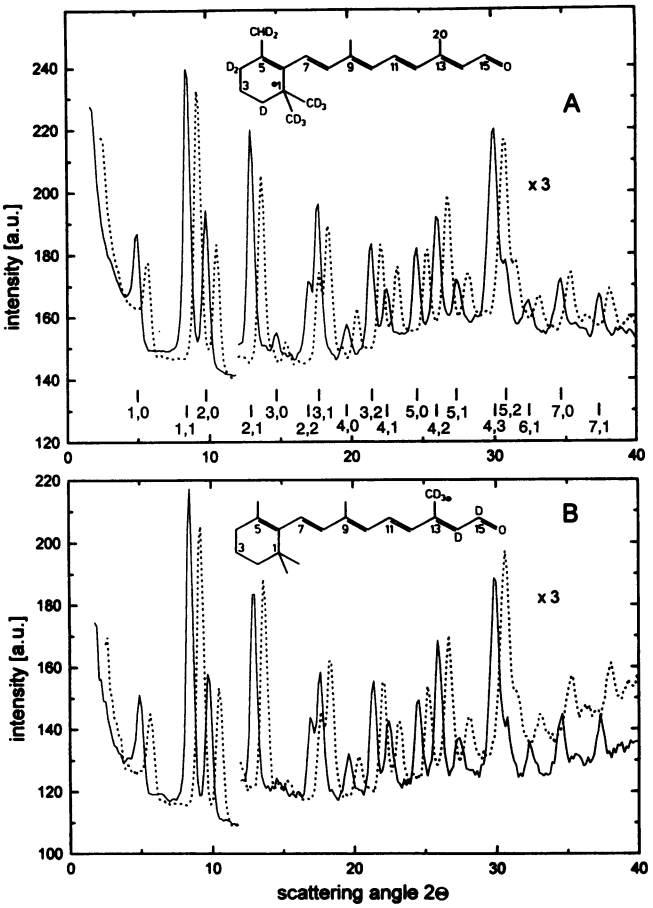

FIG. 1. (*A*) Neutron diffraction patterns for BR regenerated with D11-retinal (—) and H11-retinal (· · ·) in the M_{412} intermediate at 90 K. Beginning with the (2,1) reflection, the vertical scale has been expanded by a factor of 3. The reflections are labeled with the (*h,k*) indices for a hexagonal lattice of unit cell dimension of 61.7 Å. For clarity the dotted data sets are slightly displaced to the right. (*B*) Neutron diffraction patterns for BR regenerated with D5-retinal (—) and H5-retinal (· · ·) in M_{412}. (*Insets*) Chemical structures of the two deuterated synthetic retinals. The positions of the deuterons are indicated by D. The center of deuteration is represented by a black dot.

Clear relative intensity changes can be discerned in Fig. 1 between the protonated and deuterated retinal sample. For example, the (3,1) reflection is larger and the (4,2) peak is smaller for D11-retinal (Fig. 1*A*). Relative differences are also apparent by visual inspection of Fig. 1*B* for D5-retinal [compare reflections (1,1) and (2,1)]. The pairwise comparison of data from samples with the same chromophore in BR_{568} and M_{412} leads to difference maps characterizing the change in protein density in the BR_{568} to M_{412} transition. For example, Fig. 2 shows the result of such an analysis using columns 6 and 8 of Table 1. Similar results are obtained when using the column pairs 2 and 4, 3 and 5, and 7 and 9. The most prominent positive and negative density changes are observed near helix G, with a second positive change near helix F. These results are in good agreement with previous work (2, 4–6) and constitute an important control experiment.

The initial positions of the deuteron labels D11 and D5 in BR_{568} and M_{412} were calculated from Fourier difference maps obtained from data such as in Fig. 1 to a resolution of 7 Å [up to reflection (7,1)]. Fig. 3 shows for example the difference density for the D5 label in BR_{568} (*A*) and M_{412} (*B*). In the upper left hand corner, the boundary of the BR structure is superimposed on the difference density. By comparing *A* and *B* in Fig. 3, a small change in position of the D5 label peak near the

FIG. 2. Difference density map between M_{412} and BR_{568} for a perprotonated sample. Both positive (—) and negative (- · -) density changes occur. The bold lines in the upper left corner represent the outer boundary of BR_{568}. The approximate positions of helices F and G are as indicated.

inner boundary of helix C is noticeable. The label coordinates from the Fourier difference maps were used as starting values in the refinement procedure (8). The results of the refinement for all four label positions and label strengths are presented in Table 2. The average ratio of the integrated density of the

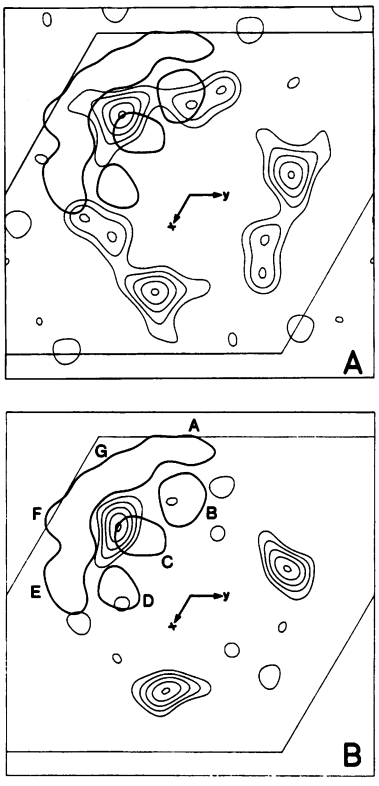

FIG. 3. Fourier difference maps for the in-plane position of the D5 label in the light-adapted ground state BR_{568} (*A*) and the photocycle intermediate M_{412} (*B*). The five contour lines shown correspond to 60%, 70%, 80%, 90%, and 99% of the positive difference density. The outer boundary of the proton density is superimposed for one of the three proteins in the unit cell (bold lines). The positions of the seven helices are labeled from A to G in *B*.

Table 2. Results of the refinement for all four label positions and label strengths

Label	x_0	y_0	A, a.u.	χ^2_ν
D11-BR_{568}	0.335	0.203	0.24	1.07
D11-M_{412}	0.323	0.200	0.30	1.15
D5-BR_{568}	0.312	0.059	0.15	1.07
D5-M_{412}	0.322	0.085	0.12	1.06

x_0, y_0 are the fractional coordinates of the label position within the unit cell (defined in Fig. 3), and A is the density of the label. The quality of the refinement is estimated by χ^2_ν (18). a.u., Arbitrary units.

refined labels is about 2:1 and is in excellent agreement with the ratio of 11:5 expected from the number of deuterons. The refined coordinates suggest a shift in the D11 position of only 0.7 Å toward helix D and for the D5 position a movement of 1.4 Å toward the β-ionone ring (Fig. 4). To analyze the significance of these changes in position, it is essential to establish proper estimates of the errors. For this purpose, Monte Carlo and model calculations were performed.

The idea of the Monte Carlo calculations is to derive new label positions with intensities, which were randomly generated within the experimental error limits, and to estimate the mean error from the distribution of the label positions. For each data set of the deuterated and protonated samples, a new set of intensities was generated as $I_{MC}(h,k) = I_{obs}(h,k) + \beta \cdot \sigma(h,k)$, where β is a $N(0,1)$ normally distributed random number and $\sigma(h,k)$ is the error of the observed intensity $I_{obs}(h,k)$. Intensities generated in this way were used in the refinement, and a new label position was calculated. The estimated value of the error in the label position is the average of the differences between 20 newly calculated positions and the position derived from the original experimental data sets. In this way, the errors in the label position were estimated to be 0.6 Å for the D11 label and 0.7 Å for the D5 label.

To obtain a further estimate of the error of the label position, we examined the probability that a model label with slightly shifted coordinates could generate the measured intensities. Models with shifted label positions within a radius of Δr = 0.5 Å, 1.0 Å, and 1.5 Å were calculated and tested with the χ^2_ν criterion (18). For each model, the mean χ^2_ν was calculated at equal Δr. From the mean χ^2_ν, the confidence level α was derived. This is the probability that the true label lies within a radius $R > \Delta r$ from the original refined label position. The numbers are given in Table 3 and lead to estimated errors in the label position of 0.5 Å for the D5 label and ≤0.5 Å for the D11 label. A shift of the D5 model label of 0.5 Å with $\alpha \approx 30\%$ is close to the 1σ error interval and is

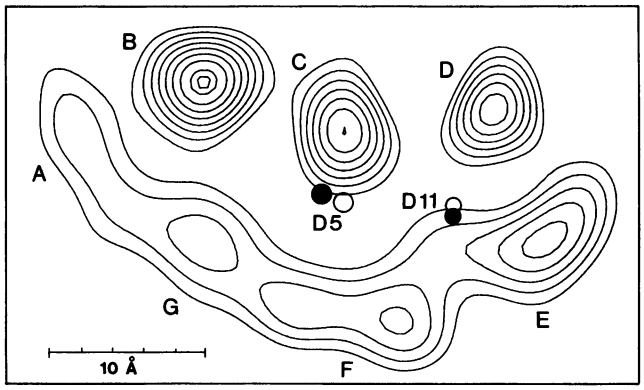

FIG. 4. Refined label positions in BR_{568} (●) and M_{412} (○) superimposed on the projected protein density. The radii of the circles indicate the estimated error of the label position. The two overlapping circles on the right correspond to the D11 label in the β-ionone ring. The two separated circles on the left represent the D5 label (mainly the C-20 methyl group).

Table 3. Confidence level α at various distances Δr from the original refined label position

Label	Δr, Å	$\overline{\chi^2_\nu}$	α, %
D11-BR_{568}	0.5	1.41	15.0
	1.0	4.06	<0.1
	1.5	4.29	<0.1
D11-M_{412}	0.5	1.35	17.0
	1.0	2.15	0.8
	1.5	3.17	<0.1
D5-BR_{568}	0.5	1.17	29.1
	1.0	1.49	9.6
	1.5	1.99	1.8
D5-M_{412}	0.5	1.18	28.4
	1.0	1.55	9.3
	1.5	2.07	1.2

α was derived from $\overline{\chi^2_\nu}$ (18).

therefore comparable to the estimated error of 0.7 Å from the Monte Carlo calculation (1σ corresponds to $\alpha = 31.7\%$). The D11 label is even better defined: a shift >0.5 Å has a probability of $\alpha = 17\%$.

Taking the average of these error estimates, we arrive at 0.6 Å for D5 and 0.55 Å for D11. The radii of the circles around the label positions in Fig. 4 correspond to these values. Since these errors occur in both BR_{568} and M_{412}, the errors in the positional changes are larger by $\sqrt{2}$. We therefore conclude that the position of the D11 label does not change in the BR_{568} to M_{412} transition (difference = 0.7 ± 0.8 Å). For the D5 label, on the other hand, with a difference of 1.4 ± 0.9 Å, we conclude that the movement is significant.

DISCUSSION

We have determined by neutron diffraction the position of the D11 and D5 labels in both the light-adapted BR_{568} state and the photocycle intermediate M_{412} under the same conditions of temperature, pH, and ionic strength. To our knowledge, this is the first time that the in-plane position of the chromophore in the light-adapted all-*trans* configuration has been measured. The measured label positions summarized in Table 2 do not differ from the results obtained with the 13-*cis*-, all-*trans*-retinal mixture of the dark-adapted BR (8, 9). Our results, presented in Fig. 4, show that the in-plane position of the β-ionone ring is within experimental error unchanged in the transition from BR_{568} to M_{412}, whereas the end of the polyene chain moves toward the ring by 1.4 ± 0.9 Å. The projected distance between the two label positions is thus shorter in M_{412}. The structural model illustrated in Fig. 5, with the conjugated chromophore perpendicular to the plane of the membrane in both the BR_{568} and M_{412} states (19–21), will be used to discuss our results. On the basis of the measured distance between the two projected label positions in BR_{568}, the polyene chain is at a 24° angle to the plane of the membrane, assuming a straight all-*trans* polyene chain and taking into account that the line between the two centers of deuteration (•) is at a 15° angle to the polyene chain. This value is slightly larger than the values of ≈20° for the transition dipole moment (22, 23). The situation is presented in Fig. 5*A*. The horizontal line represents the plane of the membrane. If we assume that in M_{412} isomerization has occurred around the C-13–C-14 double bond with the chain from C-5 to C-13 remaining fixed, it is apparent from Fig. 5*B* that the in-plane projection of the center of deuteration is very nearly the same for both BR_{568} and M_{412}. An increased tilt angle of the polyene chain from 24° in BR_{568} to 35° in M_{412} leads to the observed shift in position of the D5 label toward the β-ionone ring by 1.4 Å (Fig. 5*C*). Due to the 13-*cis* configuration, the line between the two centers of deuteration is at a 14° angle to the polyene chain in M_{412}. We conclude

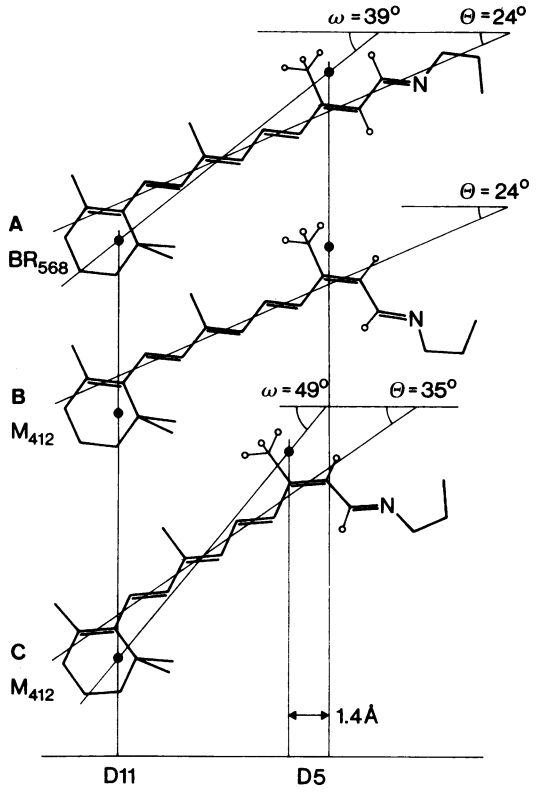

FIG. 5. Planar carbon backbone of the retinal chromophore in BR_{568} and M_{412}. The plane of the drawing is perpendicular to the plane of the membrane, represented by the horizontal line at the bottom. In BR_{568} the polyene chain tilts out of the plane of the membrane by 24° (*A*). The two centers of deuteration are marked by solid circles. The five deuterons of the D5-retinal are represented by the small open circles. In *B* it is assumed that the polyene chain in M_{412} has the same tilt as in BR_{568}. The isomerization around the C-13–C-14 bond does not alter the projected position of the label (vertical line through solid circle). In *C* the polyene chain from C-5 to C-13 tilts out of the membrane by 35° (+11° toward the cytoplasmatic surface), leading to a movement of the projected label position by 1.4 Å to the left.

that, as the combined result of isomerization and subsequent protein relaxation, the polyene chain tilts out of the plane of the membrane by about 11°, with the C-20 methyl group moving toward the cytoplasmic side of the membrane. The error in this angle is about 6°. The direction of this chromophore movement is supported by measurements of steady-state (24) and time-resolved (25, 26) linear dichroism, which show that in M_{412} the optical transition dipole moment tilts out of the plane of the membrane by about 3° and which provide a lower bound for the change in tilt angle of the polyene chain itself.

NMR experiments (27) show that trapping at low temperature and alkaline pH in the presence of Gdn·HCl leads to an M state that is 13-*cis* and C=N *anti*, just like the configuration of M_{412} in aqueous suspension under normal conditions and in the absence of Gdn·HCl. At room temperature, in a purple membrane suspension at pH 9.4 and in the presence of 1 M Gdn·HCl, BR is still active as a proton pump (2). The change in protein density in M_{412} observed here (Fig. 2) and previously (2) in the presence of Gdn·HCl is the same as that observed by x-ray diffraction (4, 5) and electron microscopy (6) in the absence of Gdn·HCl. Taken together these arguments support the view that under the conditions of our experiment an M intermediate was trapped that is similar, if not identical, to that in the absence of Gdn·HCl.

The interpretation of our data in Fig. 5*C* assumed that the polyene chain was straight in the all-*trans* form. The crystal

structure of the imidium salt of retinal shows, however, that the chain has some in-plane curvature (28), and there is evidence that this is also the case for the chromophore of BR_{568} (29). The chromophore may also exhibit some out-of-plane twist (10, 21). Whereas out-of-plane twist is not expected to change the projected length of the chain, an increase in in-plane curvature may also shorten the projected distance between the two label positions and may thus provide an alternate explanation for our experimental results.

The observed light-triggered increase in the tilt of the polyene chain and the concomitant movement of the Schiff base might be of relevance for the pumping mechanism. Besides the function of the retinal chromophore as an antenna for photon absorption, it seems to act as a molecular switch, regulating the proton accessibility to the extra- and intracellular proton translocation pathways.

This research has benefited from the excellent instrumental facilities available at the Institute Laue-Langevin (Grenoble), where the neutron diffraction experiments were performed. We thank Dr. E. Pebay Peyroula for her support as the local contact on the D16 diffractometer. This work was supported by Grants 03-HE3 FUB-6 (M.P.H.) and 03-BU3 FUB (G.B.) from the Bundesministerium für Forschung und Technologie and by Grants SFB312/B1 (M.P.H.) and SFB312/B4 (N.A.D.) from the Deutsche Forschungsgemeinschaft.

1. Dencher, N. A., Dresselhaus, D., Maret, G., Papadopoulos, G., Zaccaï, G. & Büldt, G. (1988) *Proc. Yamada Conf.* **21,** 109–115.
2. Dencher, N. A., Dresselhaus, D., Zaccaï, G. & Büldt, G. (1989) *Proc. Natl. Acad. Sci. USA* **86,** 7876–7879.
3. Dencher, N. A., Heberle, J., Bark, C., Koch, M. H. J., Rapp, G., Oesterhelt, D., Bartels, K. & Büldt, G. (1991) *Photochem. Photobiol.* **6,** 881–887.
4. Koch, M. H. J., Dencher, N. A., Oesterhelt, D., Plöhn, H.-J., Rapp, G. & Büldt, G. (1991) *EMBO J.* **10,** 521–526.
5. Nakasako, M., Kataoka, M., Amemiya, Y. & Tokunaga, F. (1991) *FEBS Lett.* **292,** 73–75.
6. Subramaniam, S., Gerstein, M., Oesterhelt, D. & Henderson, R. (1993) *EMBO J.* **12,** 1–8.
7. Seiff, F., Wallat, I., Ermann, P. & Heyn, M. P. (1985) *Proc. Natl. Acad. Sci. USA* **82,** 3227–3231.
8. Seiff, F., Westerhausen, J., Wallat, I. & Heyn, M. P. (1986) *Proc. Natl. Acad. Sci. USA* **83,** 7746–7750.
9. Heyn, M. P., Westerhausen, J., Wallat, I. & Seiff, F. (1988) *Proc. Natl. Acad. Sci. USA* **85,** 2146–2150.
10. Büldt, G., Konno, K., Nakanishi, K., Plöhn, H.-J., Rao, B. N. & Dencher, N. A. (1991) *Photochem. Photobiol.* **54,** 873–879.
11. Henderson, R., Baldwin, J. M., Ceska, T. A., Zemlin, F., Beckmann, E. & Downing, K. H. (1990) *J. Mol. Biol.* **213,** 899–929.
12. Hauß, T., Grzesiek, S., Otto, H., Westerhausen, J. & Heyn, M. P. (1990) *Biochemistry* **29,** 4904–4913.
13. Henderson, R., Baldwin, J. M., Downing, K. H., Lepault, J. & Zemlin, F. (1986) *Ultramicroscopy* **19,** 147–178.
14. Glaeser, R. M., Baldwin, J., Ceska, T. A. & Henderson, R. (1986) *Biophys. J.* **50,** 913–920.
15. Draheim, J. E. & Cassim, J. Y. (1985) *Biophys. J.* **47,** 497–507.
16. Frankel, R. D. & Forsyth, J. (1985) *Biophys. J.* **47,** 387–393.
17. Zimányi, L., Tokaji, Z. & Dollinger, G. (1987) *Biophys. J.* **51,** 145–148.
18. Bevington, P. R. (1969) *Data Reduction and Error Analysis for the Physical Sciences* (McGraw-Hill, New York).
19. Earnest, T. N., Roepe, P., Braiman, M. S., Gillespie, J. & Rothschild, K. J. (1986) *Biochemistry* **25,** 7793–7798.
20. Urabe, H., Otomo, J. & Ikegami, A. (1989) *Biophys. J.* **56,** 1225–1228.
21. Fahmy, K., Siebert, F., Grossjean, M. F. & Tavan, P. (1989) *J. Mol. Struct.* **214,** 257–288.
22. Heyn, M. P., Cherry, R. J. & Müller, U. (1977) *J. Mol. Biol.* **117,** 607–620.
23. Lin, S. W. & Mathies, R. A. (1989) *Biophys. J.* **56,** 653–660.
24. Schertler, G. F. X., Lozier, R., Michel, H. & Oesterhelt, D. (1991) *EMBO J.* **10,** 2353–2361.
25. Otto, H. & Heyn, M. P. (1991) *FEBS Lett.* **293,** 111–114.
26. Heyn, M. P. & Otto, H. (1992) *Photochem. Photobiol.* **56,** 1105–1112.
27. Smith, S. O., Courtin, J., van den Berg, E., Winkel, C., Lugtenburg, J., Herzfeld, J. & Griffin, R. G. (1989) *Biochemistry* **28,** 237–243.
28. Santarsiero, B. D., James, M. N. G., Mahendran, M. & Childs, R. F. (1990) *J. Am. Chem. Soc.* **112,** 9416–9418.
29. Ulrich, A. S., Watts, A., Wallat, I. & Heyn, M. P. (1994) *Biochemistry* **33,** 5370–5375.